Acetylthiocholine Binds to Asp74 at the Peripheral Site of Human Acetylcholinesterase as the First Step in the Catalytic Pathway†

William D. Mallender, Tivadar Szegletes, and Terrone L. Rosenberry*

Department of Pharmacology, Mayo Foundation for Medical Education and Research, and Department of Research, Mayo Clinic Jacksonville, Jacksonville, Florida 32224

Received February 1, 2000; Revised Manuscript Received April 10, 2000

ABSTRACT: Studies of ligand binding to acetylcholinesterase (AChE) have demonstrated two sites of interaction. An acyl−enzyme intermediate is formed at the acylation site, and catalytic activity can be inhibited by ligand binding to a peripheral site. The three-dimensional structures of AChE−ligand complexes reveal a narrow and deep active site gorge and indicate that ligands specific for the acylation site at the base of the gorge must first traverse the peripheral site near the gorge entrance. In recent studies attempting to clarify the role of the peripheral site in the catalytic pathway for AChE, we showed that ligands which bind specifically to the peripheral site can slow the rates at which other ligands enter and exit the acylation site, a feature we called steric blockade [Szegletes, T., Mallender, W. D., and Rosenberry, T. L. (1998) *Biochemistry 37*, 4206−4216]. We also demonstrated that cationic substrates can form a low-affinity complex at the peripheral site that accelerates catalytic hydrolysis at low substrate concentrations but results in substrate inhibition at high concentrations because of steric blockade of product release [Szegletes, T., Mallender, W. D., Thomas, P. J., and Rosenberry, T. L. (1999) *Biochemistry 38*, 122−133]. In this report, we demonstrate that a key residue in the human AChE peripheral site with which the substrate acetylthiocholine interacts is D74. We extend our kinetic model to evaluate the substrate affinity for the peripheral site, indicated by the equilibrium dissociation constant K_S, from the dependence of the substrate hydrolysis rate on substrate concentration. For human AChE, a K_S of 1.9 ± 0.7 mM obtained by fitting this substrate inhibition curve agreed with a K_S of 1.3 ± 1.0 mM measured directly from acetylthiocholine inhibition of the binding of the neurotoxin fasciculin to the peripheral site. For *Torpedo* AChE, a K_S of 0.5 ± 0.2 mM obtained from substrate inhibition agreed with a K_S of 0.4 ± 0.2 mM measured with fasciculin. Introduction of the D*72*G mutation (corresponding to D74G in human AChE) increased the K_S to 4−10 mM in the *Torpedo* enzyme and to about 33 mM in the human enzyme. While the turnover number k_{cat} was unchanged in the human D74G mutant, the roughly 20-fold decrease in acetylthiocholine affinity for the peripheral site in D74G resulted in a corresponding decrease in k_{cat}/K_{app}, the second-order hydrolysis rate constant, in the mutant. In addition, we show that D74 is important in conveying to the acylation site an inhibitory conformational effect induced by the binding of fasciculin to the peripheral site. This inhibitory effect, measured by the relative decrease in the first-order phosphorylation rate constant k_{OP} for the neutral organophosphate 7-[(methylethoxyphosphonyl)oxy]-4-methylcoumarin (EMPC) that resulted from fasciculin binding, decreased from 0.002 in wild-type human AChE to 0.24 in the D74G mutant.

The primary physiological role acetylcholinesterase (AChE)[1] is to hydrolyze the neurotransmitter acetylcholine at cholinergic synapses (*1*). AChE is one of the most efficient enzymes known (*2*), and recent studies have focused on the structural basis of its high catalytic efficiency. Ligand binding studies (*3*) and X-ray crystallography (*4*) revealed a narrow active site gorge some 20 Å deep with two separate ligand binding sites. The acylation site at the bottom of the gorge contains residues involved in a catalytic triad (H*440*, E*327*, and S*200*)[2] and W*84*, which binds to the trimethylammonium group of acetylcholine. The peripheral site at the mouth of the gorge includes, among others, residue W*279*. AChE, like other members of the α/β-hydrolase family, contains an ω-loop with boundaries set by a disulfide bond (C*67*−C*94*) (*5*, *6*). Residues from Y*70* through W*84* in this loop extend along one side of the gorge from the peripheral site to the acylation site. This segment includes residue D*72*, which is positioned near a constriction at the boundary between the peripheral site and the acylation site.

† This work was supported by Grant NS-16577 from the National Institutes of Health, Grant DAMD 17-98-2-8019 from the United States Army Medical Research Acquisition Activity, and by grants from the Muscular Dystrophy Association of America. W.D.M. was supported by a Kendall-Mayo Postdoctoral Fellowship.

* To whom correspondence should be addressed. Telephone: (904) 953-7375. Fax: (904) 953-7370. E-mail: rosenberry@mayo.edu.

[1] Abbreviations: AChE, acetylcholinesterase; TcAChE, acetylcholinesterase from *Torpedo californica*; BChE, butyrylcholinesterase; DTNB, 5,5′-dithiobis(2-nitrobenzoic acid); OP, organophosphate; EMPC, 7-[(methylethoxyphosphonyl)oxy]-4-methylcoumarin; DEPQ, 7-[(diethoxyphosphoryl)oxy]-1-methylquinolinium iodide; TMTFA, *m*-(*N*,*N*,*N*-trimethylammonio)trifluoroacetophenone.

[2] Throughout this paper, italicized residue numbers refer to the *Torpedo* AChE sequence. D74 in the human and mouse AChE sequences corresponds to D*72* in *Torpedo* AChE and D70 in mammalian BChE.

10.1021/bi000210o CCC: $19.00
Published on Web 06/08/2000

In a series of recent publications, we have focused on clarifying the role of the peripheral site in the catalytic pathway for AChE (*7*−*9*). The three-dimensional structure indicates that ligands specific for the acylation site must first pass through the peripheral site on their way to the acylation site. Other cationic ligands, including the phenanthridium derivative propidium and the fasciculins, a family of nearly identical snake venom neurotoxins, are specific for the peripheral site and do not proceed further. Cationic substrates such as the acetylcholine analogue acetylthiocholine partially competed with fasciculin for binding to the peripheral site (*8*). This discovery revealed that acetylthiocholine had a modest affinity for the peripheral site, and further kinetic analysis indicated that the binding of acetylthiocholine to the peripheral site accelerated hydrolysis rates at low substrate concentrations. The acceleration is probably the most important contribution of the peripheral site to the catalytic process. Additional information about the peripheral site was obtained by studying the formation of ternary complexes with AChE. Such complexes, involving the binding of different ligands to the acylation and peripheral sites, exhibited little thermodynamic interaction between the bound ligands (*3*). However, the binding of small cationic ligands such as propidium to the peripheral site slowed the rate constants for ligand entry into and exit from the acylation site by factors of up to 400 (*7*). We termed this effect steric blockade and demonstrated that it was responsible for pronounced propidium inhibition when substrate hydrolysis is near diffusion-controlled. Steric blockade also was shown to be involved in the phenomenon of substrate inhibition (*10*), a decrease in hydrolysis rates at high substrate concentrations. Our analysis revealed that substrate inhibition occurs because the binding of acetylthiocholine in the peripheral site also slows the rate of dissociation of product thiocholine from the acylation site, making it rate-limiting at high substrate concentrations (*8*). Steric blockade by a peripheral site ligand is preicted to result in little inhibition of substrates, like organophosphates, that equilibrate with the acylation site before reacting, and experimental data confirmed this point (*9*).

In this report, we examine the location of acetylthiocholine binding in the AChE peripheral site. A clue to this location was provided when acetylthiocholine was observed to only partially compete with fasciculin for binding to the peripheral site (*8*). This finding was unexpected, since propidium appears to be completely competitive with both fasciculin (*11*) and acetylthiocholine (*8*) at the peripheral site, and crystal structures of the fasciculin−AChE complex show direct fasciculin contacts with W*279* and most other residues in the peripheral site (*12*, *13*). However, the crystal structures also showed that D*72* was a little too deep in the gorge to make direct contact with fasciculin, and it appears possible that acetylthiocholine could bind near D*72* and still allow a nearly normal fasciculin association reaction with the remainder of the peripheral site. Furthermore, site-directed mutagenesis has identified D*72* as an important residue in the catalytic pathway. The mouse and human D74N[2] AChE mutants showed significant reductions in both k_{cat}/K_{app} for acetylthiocholine (*14*, *15*) and the second-order phosphorylation rate constant k_{OP}/K_{OP} for cationic organophosphates (*16*) relative to those of wild-type AChE, and substrate inhibition was nearly abolished in this mouse mutant (*14*). D70G[2] is a naturally occurring mutation in human butyrylcholinesterase (BChE), a close relative of AChE, that results in large increases in K_{app} for butyrylthiocholine and succinyldithiocholine relative to that of wild-type BChE (*17*). Individuals with this BChE mutation have severe difficulty in metabolizing the muscle relaxant succinyldicholine (*18*, *19*).

To examine the possibility that acetylthiocholine binds near D*72*, we constructed the human D74G mutant and assessed its ability to bind acetylthiocholine at the peripheral site both from the substrate inhibition profile and with the fasciculin competition assay. Similar analyses were carried out with wild-type *Torpedo* AChE and its D*72*G mutant to assess the importance of D*72* in acetylthiocholine binding at the peripheral site in AChE from another species. We also measured the effects of bound fasciculin on the organophosphorylation of human D74G. Fasciculin is the only peripheral site ligand identified to date that inhibits reactions at the acylation site by a mechanism in addition to steric blockade or simple steric overlap in the ternary complex. This mechanism, which appears to involve a conformational change in the acylation site, is best revealed by determination of the organophosphorylation rate constants (*9*), and we examined the extent to which it is disrupted in the D74G mutant.

EXPERIMENTAL PROCEDURES

Materials. Recombinant human "wild-type" AChE was expressed as a secreted dimeric form in *Drosophila* S2 cells in culture (*9*) and purified by two cycles of affinity chromatography on acridinium resin (*20*). AChE from *Torpedo* (type H), modified by site-directed mutagenesis as described previously (*21*) and produced by transfection of COS-7 cells with the pEF-Bos vector (*22*), was provided by S. Bon and J. Massoulié at the Ecole Normale Supérieure in Paris, France. The free cysteine (C231) was replaced by a serine, and a stop codon was introduced at position 540, thus deleting the GPI addition signal but retaining a C-terminal cysteine that results in a soluble disulfide-linked dimeric enzyme. In this study, this enzyme is denoted wild-type *Torpedo* AChE and is compared to its D*72*G derivative. *Torpedo* wild-type and D*72*G AChEs also were purified by affinity chromatography on acridinium resin except where noted. Purification did not alter the fitted substrate inhibition parameters for the *Torpedo* D*72*G enzyme (data not shown). Fasciculin 2 was obtained from C. Cervenansky at the Instituto de Investigaciones Biologicas, Clementa Estable, Montevideo, Uruguay (*11*), while fasciculin 3 was obtained from P. Marchot at the Laboratoire de Biochimie, Faculté de Médicine, Université d'Aix-Marseille II, Marseille, France (*23*). The concentration of purified fasciculin 2 was determined by absorbance ($\epsilon_{276} = 4900\ M^{-1}\ cm^{-1}$; *24*), while the fasciculin 3 concentration was determined by titration with a known amount of human erythrocyte AChE as described in ref *11*. DEPQ and EMPC were synthesized as previously described (*9*). Propidium iodide was purchased from Calbiochem.

Mutagenesis of Recombinant Human AChE. The secreted dimeric form of human AChE with a truncation sequence, including a stop codon inserted just downstream from the exon 4−5 boundary, was used as a template for mutagenesis (*9*). D74G AChE was constructed using the Alter Sites II *in vitro* Mutagenesis System (Promega Corp., Madison, WI). Briefly, the gene cassette encoding human AChE was cloned

from the *Drosophila* expression vector pPac into the cloning and mutagenesis vector pALTER to make $pALT_{human}$. DNA was transformed into JM109 *Escherichia coli* cells for preparation of phagemid ssDNA using R408 helper phage. dsDNA was synthesized *in vitro* using the AChE vector ssDNA template, DNA polymerase, DNA ligase, and three site-specific oligonucleotides. The first two oligonucleotides (provided in the Altered Sites II kit) were annealed with antibiotic resistance genes on the $pALT_{human}$ plasmid, switching the antibiotic resistance encoded on the synthesized DNA strand and allowing for selection of *E. coli* with mutant plasmids. The third oligonucleotide (synthesized by the Mayo Clinic Rochester Molecular Biology Core Facility) was annealed with AChE DNA corresponding to amino acid residues *67*−*76* to introduce the D74G mutation (GAC → GGC). The mutagenic oligonucleotide also contained a silent mutation that removed a Van91I restriction endonuclease site as a marker to confirm the presence of the mutation. The pool of mutant and wild-type dsDNA was transformed into ES 1301 mutS *E. coli*, and cultures were grown in liquid media with the appropriate antibiotic for mutant DNA selection. Plasmid DNA was prepared from these cultures and propagated in JM109 *E. coli*. Mutant plasmids from JM109 colonies were identified (after further antibiotic selection) by Van91I endonuclease digestion of purified DNA. The D74G AChE sequence was confirmed by DNA sequencing carried out at the Mayo Clinic Rochester Molecular Biology Core Facility. The modified human AChE D74G cassette was returned to the pPac vector for transfection into and expression from *Drosophila* S2 cells in tissue culture (*9*). D74G AChE was purified from culture medium by two cycles of affinity chromatography on acridinium resin (*20*). The affinity chromatography procedure was modified in that NaCl concentrations used during the washing steps did not exceed 100 mM and the Triton X-100 level was reduced to 0.02% to prevent excess stripping of bound protein off the column. Purified recombinant AChE samples analyzed by SDS−PAGE (*25*) showed no contaminants.

Steady-State Measurements of AChE-Catalyzed Substrate Hydrolysis. Hydrolysis of acetylthiocholine was monitored with a spectrophotometric Ellman assay (*26*). Assay solutions included 0.33 mM DTNB, and hydrolysis was monitored by formation of the thiolate dianion of DTNB at 412 nm [$\Delta\epsilon_{412} = 14.15$ mM^{-1} cm^{-1} (*27*)]. Hydrolysis rates v were measured at various substrate (S) concentrations in 20 mM sodium phosphate and 0.02% Triton X-100 (pH 7.0) at 25 °C, and the constant ionic strength was maintained with 0−100 mM NaCl (*8*). The dependence of v on S concentration was fitted to eq 1, the Haldane equation for substrate inhibition (*28*), by weighted nonlinear regression analysis (assuming constant percent error in v) with Fig.P (BioSoft, version 6.0). In eq 1, $V_{max} = k_{cat}[E]_{tot}$, where k_{cat} is the maximal substrate turnover rate, $[E]_{tot}$ is the total concentration of AChE active sites, K_{SS} is the substrate inhibition constant, and K_{app} is the apparent Michaelis constant. Active site concentrations were determined from V_{max}/k_{cat}, and k_{cat} was established in titrations with DEPQ monitored by fluorometric or inactivation assays (*9*). Measurements of k_{cat} at pH 7.0 for human erythrocyte AChE [$(5.78 \pm 0.38) \times 10^3$ s^{-1}, $n = 3$], wild-type recombinant human AChE [$(6.61 \pm 0.32) \times 10^3$ s^{-1}, $n = 3$], and D74G human AChE [$(6.53 \pm 0.27) \times 10^3$ s^{-1}, $n = 3$] were not significantly different, and a mean k_{cat} value of 6.3×10^3 s^{-1} was assumed. This value agrees with a previously assigned k_{cat} of 7×10^3 s^{-1} at pH 8.0 (*8*) and a pK_a of 6.3 for k_{cat} (*20*). Determinations of k_{cat} at pH 7.0 for wild-type recombinant *Torpedo* AChE [$(4.18 \pm 0.20) \times 10^3$ s^{-1}, $n = 3$] and D*72*G *Torpedo* AChE [$(5.33 \pm 0.17) \times 10^3$ s^{-1}, $n = 3$] also were averaged to give a mean k_{cat} value of 4.8×10^3 s^{-1}.

$$v = \frac{V_{max}[S]}{[S]\left(1 + \frac{[S]}{K_{SS}}\right) + K_{app}} \quad (1)$$

Determination of Rate Constants in Scheme 3. We have recently presented substantial evidence which shows that catalysis of acetylthiocholine hydrolysis by human AChE proceeds according to Scheme 3 in the Results (*8*). To estimate key rate constants in Scheme 3, we solved the corresponding steady-state rate equations numerically with the program SCoP (version 3.51) (*7*, *8*). This solution avoids equilibrium assumptions and allows examination of Scheme 3 in the context of our steric blockade model, which postulates that $k_{-P2} < k_{-P}$ and $a = b = 1$. To allow the fitting of rate constants from data, our current treatment also simplifies Schemes 2 and 3 from their more general format (see ref *8*) by postulating that product P bound to the acylation site does not alter the rate constant for deacetylation, that rate constants for P dissociation from the acetylated enzyme are identical to those from free enzyme, and that peripheral site binding is unaffected by the binding of ligands to the acylation site. These assumptions still leave eight rate constants in Scheme 3 to be assigned or determined. On the basis of previous experimental data, we assigned $k_2 = k_3$ (*7*, *29*) and $k_{-P2}/k_{-P} = 0.01$ (*7*, *8*). Additional constraints placed upon the remaining parameters are given by the following three equations. The second-order substrate hydrolysis rate constant k_{cat}/K_{app} for Schemes 2 and 3 is given by eq 2.

$$\frac{k_{cat}}{K_{app}} = \frac{k_S k_1 k_2}{k_{-S}k_{-1} + k_2(k_{-S} + k_1)} \quad (2)$$

An adjustable constant B is defined in eq 3 to set the ratio of k_S equal to k_{cat}/K_{app}.

$$B = \frac{k_S K_{app}}{k_{cat}} \quad (3)$$

Another adjustable constant R/R_S is defined in eq 4.

$$\frac{R}{R_S} = 1 + \frac{1.5\,(B - 1)}{B\left(1 + \frac{k_2}{k_{-1}}\right)} \quad (4)$$

To solve for the parameters in Scheme 3, k_{cat} was set to the

human or *Torpedo* AChE value determined above and K_{app} and $[E]_{tot}$ were obtained by an initial fit of data to eq 1. Values of B and R/R_S were assigned, and the dependence of v on [S] was then fitted in the SCoP program for the three remaining parameters in Scheme 3: $K_S = k_{-S}/k_S$, k_{-P}, and k_2. The three other rate constants (k_1, k_{-1}, and k_{-S}) were calculated iteratively from eqs 2−4 during the fitting of these parameters.

The constants B and R/R_S were defined for the fitting procedure outlined here because they are constrained within a narrow range of values (*8*). According to eq 2, $B \geq 1$. When $B \cong 1$, $k_{cat}/K_{app} \cong k_S$ and the second-order reaction is diffusion-controlled (i.e., $k_{-S}/k_1 \cong 0$). For acetylthiocholine, the relatively high value of k_{cat}/K_{app} ($>10^8$ M^{-1} s^{-1}; see ref *8*) and its viscosity dependence (*30*) argue that B is close to 1, and it is very unlikely to exceed 10. According to eq 4, $1 \leq R/R_S \leq 2.5$. This range places no restriction on the value of k_2/k_{-1}, but via assignment of B and R/R_S, the value of k_2/k_{-1} is set by eq 4 and that of k_{-S}/k_1 by eqs 2 and 3. R and R_S are introduced because they represent observed solvent deuterium oxide isotope effects for AChE. If k_2 and k_S are the only intrinsic rate constants in eq 2 that are altered when H_2O is replaced with D_2O, and R, R_S, and R_2 are defined as the respective ratios of k_{cat}/K_{app}, k_S, and k_2 in H_2O to that in D_2O, then R/R_S is given by eq 4 when R_2 is assigned a typical value of 2.5 (*8*). For all data fitting here, B was estimated to be 1.2 and R/R_S was set at the observed value of 1.1 (*8*). However, varying these constants over their entire range ($1 \leq B \leq 10$ and $1 \leq R/R_S \leq 2.5$), while producing large changes in calculated k_2/k_{-1}, resulted in no more than 40% changes in the fitted parameters K_S, k_{-P}, and k_2 for wild-type AChE.[3] Depending on the initial values of these three parameters, simultaneous fitting of wild-type AChE activities as in Figure 1A converged on one of two alternative solutions. The solution where $k_{-P} > k_2$ was selected, consistent with previous estimates of k_{-P} (*8*).

Slow Equilibration of Fasciculin in the Presence of Peripheral Site Inhibitors. Apparent association rate constants k_{on} for fasciculin binding to the AChE peripheral site were measured by a procedure used previously (*8*, *11*). In brief, stock solutions of fasciculin 2 (140 μM) and fasciculin 3 (20 nM) were prepared in buffer [20 mM sodium phosphate and 0.02% Triton X-100 (pH 7.0)] and contained 0.1% bovine serum albumin (*11*). Association reactions (0.1 mL for fasciculin 3 and 1−2 mL for fasciculin 2) were initiated by adding small volumes of AChE and acetylthiocholine to final concentrations of 0.1−1.8 nM fasciculin 2 (*Torpedo* AChE) or 1−5 nM fasciculin 3 (human AChE) and 0.1−30 mM acetylthiocholine. The reaction mixtures also included 0.1 mM DTNB and NaCl (with a NaCl concentration of 60 mM − [S]) in buffer at 25 °C. Fasciculin binding was assessed under approximate first-order conditions in which the fasciculin concentration was at least 7 times higher than the concentration of AChE and acetylthiocholine was not significantly depleted (<20%). Acetylthiocholine hydrolysis rates v determined over 2 s intervals were fitted by nonlinear regression analysis (BioSoft Fig.P) to eq 5.

$$v = v_{final} + (v_{initial} - v_{final})\, e^{-kt} \quad (5)$$

In eq 5, $v_{initial}$ and v_{final} are the calculated values of v at time zero and at the final steady state when fasciculin binding has reached equilibrium, respectively, and k is the observed first-order rate constant for the approach to the final steady state. Each series of binding measurements included reactions at a fixed acetylthiocholine (S) concentration and four to ten fasciculin concentrations [F]. The observed k for each reaction was given by eq 6, and k_{on}, the apparent association rate constant, was determined by linear regression analysis in which k values were weighted by the reciprocal of their variance.

$$k = k_{on}[F] + k_{off} \quad (6)$$

If ligand binding to the peripheral site is unaffected by the presence of ligands or an acyl group at the acylation site, then only two sets of enzyme species in Scheme 3 below need be considered, $\Sigma E[S_P]$ and ΣE (*8*). These are the sums of the concentrations of all enzyme species in which S or nothing, respectively, is bound to the peripheral site. Assuming that fasciculin reacts with species in ΣE with an intrinsic association rate constant k_F and with species in $\Sigma E[S_P]$ with an intrinsic association rate constant k_{FP}, k_{on} is given by eq 7, where K_S is the equilibrium dissociation constant for S at the peripheral site (*8*).

$$k_{on} = \frac{k_F + k_{FP}\dfrac{[S]}{K_S}}{1 + \dfrac{[S]}{K_S}} \quad (7)$$

To obtain estimates of K_S, values of k_{on} obtained at each S concentration were fitted to eq 7 by nonlinear regression analysis (BioSoft Fig.P) in which k_{on} values were weighted by the reciprocal of their variance.

Phosphorylation of Human D74G AChE by Fluorogenic OPs. Reaction of recombinant human D74G AChE with EMPC or DEPQ was monitored by the appearance of their fluorescent leaving groups by stopped flow fluorometry as described previously for wild-type human AChEs (*9*). We have shown that direct fluorescence monitoring of the leaving group during phosphorylation avoids misinterpretations of fasciculin inhibition that arise when phosphorylation is assessed by enzyme inactivation (*9*). The misinterpretation resulted from a small population of AChE that was resistant to normal fasciculin inhibition and dominated the enzyme activity during OP inactivation measurements in the presence of fasciculin. Measurements of inactivation of the D74G mutant by EMPC and DEPQ in the absence of fasciculin again indicated more than one population of enzyme. Stoichiometric titration of the D74G stock with DEPQ in the presence of fasciculin (*9*) indicated that less than 10% corresponded to the fasciculin-resistant population (data not shown).

Fluorogenic phosphorylation reactions were conducted in 20 mM sodium phosphate and 0.02% Triton X-100 at 23

[3] Values of B and R/R_S have a greater effect on the fitted parameters when little substrate inhibition is observed. When k_2 was fixed for the human D74G data sets in Table 1, fitted values of K_S and k_{-P} remained within a factor of 2 of those shown over most of the range of B and R/R_S values. However, in certain narrow ranges (e.g., $1.00 < R/R_S < 1.02$ and $1.3 < B < 1.8$, or $2 < R/R_S$ and $4 < B < 8$), fitted values of K_S and k_{-P} differed by up to a factor of 10.

°C (pH 8.0 for EMPC and pH 7.0 for DEPQ). The release of product from each OP occurred in two phases, a large rapid phase and a small slower phase, and was fitted to an equation with two exponential terms (*9*). Some reactions included the peripheral site inhibitors propidium (150 μM) or fasciculin 2 (10 μM). A two-exponential fit also was required with DEPQ in the presence of propidium. Additional precautions were taken with fasciculin (*9*). The rate constants k for the rapid phase were analyzed according to Scheme 1.

Scheme 1

$$\begin{array}{ccccccc} \mathrm{OPX} + E & \overset{K_O}{\rightleftharpoons} & E\mathrm{OPX} & \overset{k_2}{\longrightarrow} & \mathrm{X} + E\mathrm{OP} & \overset{k_3}{\longrightarrow} & E + \mathrm{OPOH} \\ + & & + & & + & & \\ \mathrm{I} & & \mathrm{I} & & \mathrm{I} & & \\ K_I \Updownarrow & & K_{SI} \Updownarrow & & K_{AI} \Updownarrow & & \\ \mathrm{OPX} + E\mathrm{I_P} & \overset{K_{O2}}{\rightleftharpoons} & E\mathrm{OPXI_P} & \overset{ak_2}{\longrightarrow} & \mathrm{X} + E\mathrm{OPI_P} & \overset{k_3}{\longrightarrow} & E\mathrm{I_P} + \mathrm{OPOH} \end{array}$$

In this scheme, OPX is the intact OP with leaving group X, *E*OPX is the initial complex of the OP with AChE, characterized by the equilibrium dissociation constant K_O which equals k_{-O}/k_O (*9*) and *E*OP is the phosphorylated enzyme. The ligand I can bind to the peripheral site in each of the enzyme species (as denoted by the subscript P**)**. OPs were assumed to equilibrate with the AChE acylation site even when inhibitors were bound to the peripheral site, and the dephosphorylation rate constant k_3 was assumed to be negligible. The dependence of k on the OP concentration was analyzed by weighted nonlinear regression analysis (assuming constant percent error in k) according to eq 8 to give k_{OP} and k_{OP}/K_{OP}, the respective first- and second-order rate constants of phosphorylation, respectively.

$$k = \frac{k_{OP}\,[\mathrm{OP}]}{K_{OP} + [\mathrm{OP}]} \tag{8}$$

In the absence of I, $k_{OP} = k_2$ and $K_{OP} = K_O$. In the presence of I, the relative intrinsic first-order rate constant a for phosphorylation in Scheme 1 was calculated from k_{OP}, K_{OP}, and the competitive inhibition constant K_I for the inhibitor as outlined previously (*9*). Values of K_I were obtained in the pH 7.0 buffer with acetylthiocholine as the substrate. The K_I for propidium was calculated from the slopes of $1/v$ versus 1/[S] plots over a range of fixed concentrations of inhibitor, while the K_I for fasciculin 2 was estimated from relative v measurements in the presence and absence of inhibitor at low S concentrations (*7*).

RESULTS

A Mechanistic Model for Substrate Inhibition of AChE. Traditional catalytic pathways for AChE propose the binding of an ester substrate S to the acylation site to form an *E*S complex, followed by formation of the acylated enzyme intermediate *E*A and deacylation to regenerate the free enzyme *E*. We recently obtained evidence that the catalytic pathway for AChE should be extended by making explicit two new classes of intermediates (*8*). One class includes enzyme species with the initial product of hydrolysis, the alcohol leaving group P (e.g., thiocholine), still bound to the acylation site. These intermediates are denoted *E*AP and *E*P in Scheme 2.

Scheme 2

$$\begin{array}{ccccccccc} & & & & \mathrm{Ac} + E\mathrm{P} & \overset{k_{-P}}{\longrightarrow} & \mathrm{P} + E & & \\ & & & & \uparrow k_3 & & & & \\ E + \mathrm{S} & \underset{k_{-S}}{\overset{k_S}{\rightleftharpoons}} & E\mathrm{S_P} & \underset{k_{-1}}{\overset{k_1}{\rightleftharpoons}} & E\mathrm{S} & \overset{k_2}{\longrightarrow} & E\mathrm{AP} & \overset{k_{-P}}{\longrightarrow} \mathrm{P} + E\mathrm{A} & \overset{k_3}{\longrightarrow} E + \mathrm{Ac} \end{array}$$

The second includes intermediates in which S is bound to the AChE peripheral site, indicated by the subscript P as in ES_P in Scheme 2. The substrate initially binds in ES_P and then slides into the acylation site to give *E*S. Previous schemes that ignore intermediates such as *E*AP and *E*P can sometimes be justified. For example, with acetylthiocholine, the product dissociation rate constant k_{-P} is estimated to be nearly an order of magnitude greater than the acylation rate constant k_2 or deacylation rate constant k_3, and explicit inclusion of *E*AP, *E*P, and k_{-P} changes calculated values of k_{cat} by less than 1% (*8*). According to Scheme 2, a plot of the substrate hydrolysis rates v against the substrate concentration [S] should fit the familiar Michaelis−Menten expression. However, AChE shows substrate inhibition and thus requires a model in which a second molecule of substrate interacts with at least one of the intermediates in Scheme 2. Our recent evidence supports Scheme 3 (*8*).

Scheme 3

$$\begin{array}{ccccccccc} & & & & \begin{array}{c}\mathrm{Ac}\\ +\\ E\mathrm{P}\end{array} & \overset{k_{-P}}{\longrightarrow} & \mathrm{P} + E & & \\ & & & & \uparrow k_3 & & & & \\ E + \mathrm{S} & \underset{k_{-S}}{\overset{k_S}{\rightleftharpoons}} & E\mathrm{S_P} & \underset{k_{-1}}{\overset{k_1}{\rightleftharpoons}} & \begin{array}{c}E\mathrm{S}\\ +\\ \mathrm{S}\\ \Updownarrow\end{array} & \overset{k_2}{\longrightarrow} & \begin{array}{c}E\mathrm{AP}\\ +\\ \mathrm{S}\\ \Updownarrow\end{array} & \overset{k_{-P}}{\longrightarrow} \mathrm{P} + \begin{array}{c}E\mathrm{A}\\ +\\ \mathrm{S}\\ \Updownarrow\end{array} & \overset{k_3}{\longrightarrow} E + \mathrm{Ac} \\ & & & & E\mathrm{SS_P} & \overset{ak_2}{\longrightarrow} & E\mathrm{APS_P} & \overset{k_{-P2}}{\longrightarrow} \mathrm{P} + E\mathrm{AS_P} & \overset{bk_3}{\longrightarrow} E\mathrm{S_P} + \mathrm{Ac} \\ & & & & \downarrow bk_3 & & & & \\ & & & & \mathrm{Ac} + E\mathrm{PS_P} & \overset{k_{-P2}}{\longrightarrow} & \mathrm{P} + E\mathrm{S_P} & & \end{array}$$

In this scheme, the second molecule of substrate can bind to the peripheral site in the *E*S, *E*A, *E*AP, and *E*P intermediates in Scheme 2 with an association rate constant k_S and a dissociation rate constant k_{-S}. In theory, substrate inhibition could arise from inhibition of acylation ($a < 1$) or of deacylation ($b < 1$) when S binds to the peripheral site, but there is no evidence that the binding of a small ligand like acetylthiocholine to the peripheral site can inhibit these steps. However, it has been directly shown that the binding of the small peripheral site ligands propidium or gallamine decreases the association and dissociation rate constants for ligand binding to the acylation site by factors of 10−400 (*7*). Substrate binding to the peripheral site then would be expected to slow the rate constant for product dissociation ($k_{-P2} < k_{-P}$) in Scheme 3. If k_{-P2} falls within the range of k_2 and k_3, then ES_P can accumulate at high substrate concentrations and result in substrate inhibition. We recently

Table 1: Comparison of K_S Values Obtained from Substrate Inhibition Curves and from Fasciculin Competition[a]

	rate constants from substrate inhibition				
AChE	*n*	K_S (mM)	k_{-P} (s^{-1})	k_2 (s^{-1})	K_S from fasciculin competition (mM)
human wild type	3	1.9 ± 0.7[b]	$(6 \pm 1) \times 10^4$[b]	$(1.28 \pm 0.02) \times 10^4$	1.3 ± 1.0
human D74G	3	33 ± 8[c]	$(9 \pm 3) \times 10^4$[c]	1.28×10^4[d]	–
Torpedo wild type	2	0.51 ± 0.16	$(16 \pm 3) \times 10^4$	$(0.97 \pm 0.01) \times 10^4$	0.40 ± 0.21
Torpedo D72G	3	10 ± 1[b]	$(4 \pm 0.3) \times 10^4$	0.97×10^4[d]	4 ± 2

[a] Rate constants from substrate inhibition were the means of *n* measurements obtained by data fitting with the SCoP program and eqs 2−4. Estimates of K_S from fasciculin competition were obtained with eq 7 as shown in Figures 1B and 2B. [b] The mean includes one experiment in which the sum of [NaCl] and [S] was 40 mM. The K_S obtained from this experiment was normalized to 60 mM prior to calculating the mean by assuming that ionic strength affected only k_S (*31*) and that k_S was inversely proportional to K_{app} (eq 3). [c] The mean includes experiments in which the sum of [NaCl] and [S] was fixed at 40, 60, or 100 mM. K_S values obtained from the experiments at 40 and 100 mM were normalized to 60 mM prior to calculating the mean as in footnote b. [d] For the fitting of K_S and k_{-P}, this k_2 was fixed at the k_2 value observed for the wild-type AChE.

examined whether this scheme could account quantitatively for substrate inhibition profiles with human erythrocyte AChE by measuring the affinity of S for the peripheral site in a fasciculin competition assay (*8*; see Figure 1B below). The value of K_S ($=k_{-S}/k_S$) obtained for acetylthiocholine was about 1 mM. This value was then combined with our steric blockade model of Scheme 3, which postulates that $k_{-P2} < k_{-P}$ but that $a = b = 1$, to construct a nonequilibrium simulation of the substrate inhibition profile that was in excellent agreement with the observed profile (*8*).

Estimation of the Acetylthiocholine Affinity for the AChE Peripheral Site Directly from the Substrate Inhibition Profile. While our previous work demonstrated that experimental estimates of some of the remaining rate constants allowed reasonable simulation of substrate inhibition plots, our goal here was to actually fit the two key kinetic parameters in Scheme 3, K_S and k_{-P}, with substrate inhibition data. To achieve this, we reduced the 11 rate constant variables in Scheme 3 to three that could be fitted, as outlined in Experimental Procedures. Briefly, the assumptions in our steric blockade model together with previous data from inhibition of substrate hydrolysis by bound peripheral site ligands (*7*) decreased the number of variables to the seven rate constants in Scheme 2. Assigning $k_3 = k_2$ (*29*) and invoking eqs 2−4 further reduced the system to three fitted parameters (K_S, k_{-P}, and k_2). The profile of v versus [S] for acetylthiocholine with recombinant wild-type human AChE exhibited the bell shape that is the hallmark of pronounced substrate inhibition, and this profile was fitted precisely by the procedure (Figure 1A). Fitted values of K_S (1.9 ± 0.7 mM) and k_{-P} [$(6 \pm 1) \times 10^4$ s^{-1}] averaged from this experiment and two others (Table 1) agreed to within 40% of the corresponding values assigned previously to simulate substrate inhibition for human erythrocyte AChE (*8*).

We selected K_S and k_{-P} as parameters to be fitted because they can be compared to independent experimentally predicted values. The predicted k_{-P} was calculated indirectly from the relationship $k_{-P} = K_P k_P$, where K_P is the measured equilibrium dissociation constant for thiocholine inhibition of AChE and the association rate constant k_P for thiocholine is assumed to be the same as k_S for acetylthiocholine. Its calculated value (1.3×10^5 s^{-1}) agreed with the simulated k_{-P} value (*8*) and the fitted k_{-P} value determined here. To obtain the predicted K_S for acetylthiocholine, we employed the fasciculin competition assay in Figure 1B. In this assay, the substrate affinity for the peripheral site is determined from the effect of substrate concentration on the rate of equilibration of fasciculin at the peripheral site. The association of fasciculin with the AChE peripheral site was monitored as a decrease in AChE activity toward acetylthiocholine (*8*). The apparent fasciculin association rate constants k_{on} then were calculated from the rate constants for this activity decrease as a function of the fasciculin concentration, and finally, the dependence of k_{on} on the acetylthiocholine concentration was fitted to eq 7 to obtain K_S. The assay requires a sufficiently low dissociation rate constant k_{-F} for the fasciculin−AChE complex to allow measurement of the initial rate constants for fasciculin association, and our preliminary observations indicated that k_{-F} for fasciculin 2 with human D74G was too high to allow these measurements. Therefore, we turned to fasciculin 3, which was reported to have a K_d nearly 100-fold smaller than that of fasciculin 2 with rat brain AChE (*23*) and which did allow k_{on} determinations with the human D74G. As observed previously for fasciculin 2 and human erythrocyte AChE (*8*), acetylthiocholine only partially blocked the association of fasciculin 3 with recombinant wild-type human AChE (Figure 1B). At high saturating concentrations of acetylthiocholine, k_{on} decreased to about 50% of its extrapolated value in the absence of acetylthiocholine. Fitting the k_{on} values for fasciculin 3 at various concentrations of acetylthiocholine to eq 7 gave a K_S of 1.3 ± 1.0 mM. The precision of the individual k_{on} points made it difficult to decrease the error of this estimate, but this K_S value agreed well with that obtained from the substrate inhibition data (Table 1).

Human AChE Residue D74 Is Important in the Binding of Acetylthiocholine to the Peripheral Site of AChE. The quantitative agreement between the K_S measured by fasciculin competition and that obtained by fitting the substrate inhibition profile provided reassuring support for our model in Scheme 3 and its application to wild-type human AChE. We next investigated whether such agreement would extend to the human D74G mutant. The rationale outlined in the introductory section for focusing on this mutant is that D74 may be the key residue in defining peripheral site binding of acetylthiocholine. If this idea is correct, K_S should increase dramatically in D74G mutants. With the human D74G enzyme in Figure 1A, the extent of substrate inhibition in fact was decreased to such an extent that the three-parameter fit in SCoP was unreliable and sometimes failed to converge with the relation $k_2 < k_{-P}$. Therefore, k_2 was fixed to the value in Table 1 obtained for the wild-type human AChE, and only K_S and k_{-P} were fitted. The assumption that k_2 is the same for human wild-type and D74G AChEs was supported by our observation that these AChEs have the same

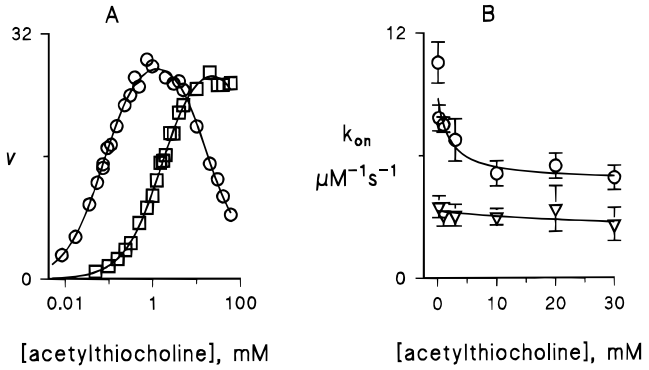

FIGURE 1: Acetylthiocholine binding to the peripheral site of human AChE. Reaction mixtures with varying amounts of acetylthiocholine were supplemented with NaCl such that [S] + [NaCl] = 60 mM to maintain a constant ionic strength. (A) Substrate inhibition with acetylthiocholine. Points represent initial velocities (micromolar per minute) measured at the indicated substrate concentrations with the wild-type (O) or D74G (□) AChE (80 pM) as outlined in Experimental Procedures. Lines were fitted with the SCoP program by employing eqs 2−4. For wild-type AChE, the parameters K_S, k_{-P}, and k_2 were fitted simultaneously, while for the D74G mutant, k_2 was fixed at 1.28×10^4 s^{-1} and K_S and k_{-P} were fitted (see Table 1). Lines fitted with the Haldane equation (eq 1) were virtually superimposable with those shown and gave a K_{app} of 76 ± 2 μM and a K_{SS} of 22 ± 1 mM for wild-type AChE and a K_{app} of 1670 ± 60 μM and a K_{SS} of 300 ± 70 mM for the D74G mutant. (B) Inhibition of fasciculin 3 binding by acetylthiocholine. Association rate constants k_{on} for fasciculin 3 measured at the indicated substrate concentrations with wild-type (○) or D74G (▽) AChE were determined by analysis with eqs 5 and 6 as outlined in Experimental Procedures (data not shown). Points represent a series of k_{on} measurements, and lines were obtained with eq 7 by fixing K_S at the value obtained from substrate inhibition in Table 1 and fitting k_{FP}/k_F to 0.52 ± 0.05 (wild type) or 0.6 ± 0.5 (D74G). A line for the wild-type AChE points fitting all three constants in eq 7 corresponded closely to that shown and gave a K_S of 1.3 ± 1.0 mM and a k_{FP}/k_F of 0.52 ± 0.06.

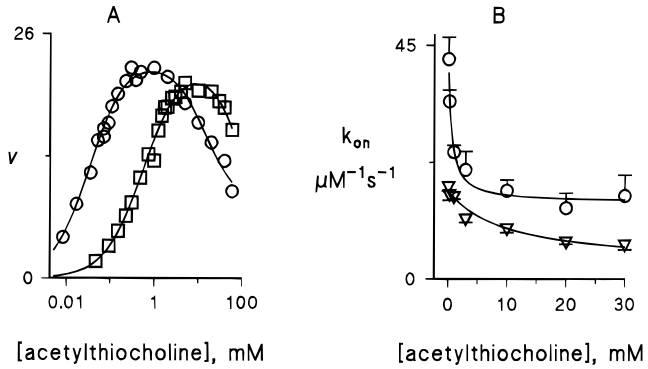

FIGURE 2: Acetylthiocholine binding to the peripheral site of *Torpedo* AChE. Ionic strength was maintained with up to 60 mM NaCl as shown in Figure 1. (A) Substrate inhibition with acetylthiocholine. Assays were conducted as described for Figure 1A with wild-type (○) or D*72*G (□) AChE (80 pM). Lines were fitted with the SCoP program as in Figure 1A except that for the D*72*G mutant k_2 was fixed at 0.97×10^4 s^{-1} (see Table 1). Lines fitted with the Haldane equation (eq 1) were close to (wild type) or virtually superimposable with (D*72*G) those shown and gave a K_{app} of 35 ± 2 μM and a K_{SS} of 39 ± 3 mM for wild-type AChE and a K_{app} of 570 ± 25 μM and a K_{SS} of 140 ± 20 mM for the D*72*G mutant. (B) Inhibition of fasciculin 2 binding by acetylthiocholine. Association rate constants k_{on} for fasciculin 2 with affinity-purified wild-type (○) or unpurified D*72*G (▽) AChE were determined as described for Figure 1B (data not shown). Lines were obtained as in Figure 1B with k_{FP}/k_F fitted to 0.33 ± 0.04 (wild type) or 0.15 ± 0.05 (D*72*G). Lines fitting all three constants in eq 7 corresponded closely to those shown and gave a K_S of 0.40 ± 0.21 mM and a k_{FP}/k_F of 0.32 ± 0.05 for the wild-type points and a K_S of 3.8 ± 1.7 mM and a k_{FP}/k_F of 0.30 ± 0.06 for the D*72*G points.

k_{cat} value (see Experimental Procedures), and k_2 is a major contributor to k_{cat}. Average fitted values of K_S (33 ± 8 mM) and k_{-P} [(9 ± 3) × 10^4 s^{-1}] were obtained from the human D74G data in Figure 1B and two additional experiments at slightly different ionic strengths (Table 1). Ionic strength had no effect on k_{-P}, which was nearly unchanged from the value for wild-type AChE. In contrast, K_S increased about 20-fold with the D74G mutant, and the change in this parameter alone was sufficient to nearly abolish substrate inhibition. Of particular importance, this increase in K_S was supported by the fasciculin 3 competition data for the human D74G mutant in Figure 1B. Values of k_{on} did not differ significantly as the acetylthiocholine concentration ranged from 0.1 to 30 mM, and the data could be fitted to eq 7 by assigning a fixed K_S of 33 mM from the substrate inhibition data.

To determine whether D*72* was essential for the binding of acetylthiocholine to the peripheral site of AChE from another species, we examined recombinant *Torpedo* AChEs. Wild-type *Torpedo* AChE exhibited substrate inhibition similar to that observed with wild-type human AChE (Figure 2A), and average fitted values of K_S (0.5 ± 0.2 mM) and k_{-P} [(16 ± 3) × 10^4 s^{-1}] were obtained (Table 1). Both the wild type and D*72*G AChEs from *Torpedo* had sufficient affinity for fasciculin 2 to conduct fasciculin competition measurements. Acetylthiocholine was slightly more effective in blocking the association of fasciculin 2 with the wild-type *Torpedo* than with the wild-type human AChE, as high saturating concentrations of acetylthiocholine decreased k_{on} to about one-third of its extrapolated value in the absence of acetylthiocholine (Figure 2B). Fitting the k_{on} values to eq 7 gave a K_S of 0.4 ± 0.2 mM (Table 1), in agreement with the K_S obtained from substrate inhibition of wild-type *Torpedo* AChE. Substrate inhibition with the *Torpedo* D*72*G mutant was more evident than with the human D74G enzyme (Figure 2A). As with human D74G, however, it was necessary to fix k_2 to obtain a K_S of 10 ± 1 mM (Table 1). The fasciculin 2 competition data supported this estimate. Values of k_{on} with the *Torpedo* D*72*G mutant decreased at least 3-fold as the acetylthiocholine concentration ranged from 0.1 to 30 mM (Figure 2B), and fitting to eq 7 gave a K_S (4 ± 2 mM). The somewhat lower K_S values for the wild-type and D*72*G *Torpedo* AChEs relative to those of the corresponding human AChEs suggest that residues other than D*72* contribute more to the peripheral site for acetylthiocholine in *Torpedo* AChE than in human AChE. For example, residues *72*−*75* in *Torpedo* AChE are DEQF, while in human AChE they are DTLY; this sequence difference may contribute to greater acetylthiocholine affinities in the peripheral site of the *Torpedo* AChEs.

The effects of the D*72*G mutation that we observe on the experimental kinetic parameters for acetylthiocholine hydrolysis in eq 1 are consistent with previous analyses of D*72* mutants of AChE. We found no significant difference in k_{cat} between human wild-type and D74G AChEs and a slight 25−30% increase in the k_{cat} for *Torpedo* D72G AChE relative to that for the *Torpedo* wild-type enzyme (see Experimental Procedures), in reasonable agreement with a small 40% decrease in the reported k_{cat} values for mouse and human D74N (*14*, *15*). All studies agree that K_{app}

Table 2: Rate Constants for the Phosphorylation of Wild-Type and D72G AChE by Fluorogenic OPs[a]

OP enzyme	inhibitor	k_{OP} (min^{-1})	a	K_{OP} (μM)	k_{OP}/K_{OP} (μM^{-1} min^{-1})	k_{OP}/K_{OP} relative decrease (fold)
EMPC						
wild type[b]						
	none	150 ± 11	−	224 ± 24	0.67 ± 0.03	−
	propidium	570 ± 140[c]	5 ± 2[c]	1260 ± 350[c]	0.45 ± 0.02	1.5
	fasciculin	0.23 ± 0.08	0.002	220 ± 110	0.0011 ± 0.0002	610
D74G						
	none	74 ± 10	−	64 ± 12	1.2 ± 0.1	−
	propidium	710 ± 110	>10	330 ± 70	2.2 ± 0.2	*d*
	fasciculin	19 ± 4	0.24 ± 0.08	1260 ± 320	0.015 ± 0.001	80
DEPQ						
wild type[b]						
	none	1600 ± 200	−	7.5 ± 1.3	205 ± 11	−
	propidium	1200 ± 400[c]	0.7 ± 0.4[c]	85 ± 30[c]	15 ± 1	14
	fasciculin	0.66 ± 0.10	0.0003	700 ± 140	0.0010 ± 0.0001	220000
D74G						
	none	850 ± 140	−	90 ± 20	10 ± 1	−
	propidium	760 ± 300[c]	0.8 ± 0.9[c]	240 ± 130[c]	3.2 ± 0.4	3
	fasciculin	*e*	*e*	*e*	<0.006 ± 0.0004	>1500

[a] Values of k_{OP} and K_{OP} were determined from the dependence of k on [OP] (eq 8), and a (Scheme 1) was calculated by extrapolation to a saturating concentration of inhibitor (*9*). [b] Data from ref *9*. [c] The maximum [OP] employed (30−60% of the estimated K_{OP}) did not exceed 80% of the estimated K_{OP}, and therefore, estimates of k_{OP} and K_{OP} are approximate. [d] k_{OP}/K_{OP} increased by a factor of 1.9. [e] No estimate was possible because of the lower affinity of fasciculin 2 for the D74G mutant, the low reactivity of the complex of fasciculin 2 and D74G with DEPQ, and the near linearity of k with [OP] (eq 8).

increases when D*72* is mutated, and our observations of a 22-fold increase in human D74G (Figure 1A) and a 16-fold increase in *Torpedo* D*72*G (Figure 2A) are consistent with 28- and 5-fold increases reported for mouse (*14*) and human (*15*) D74N, respectively. We also found that K_{SS}, the experimental substrate inhibition constant, increased by factors of 14 with human D74G and 4 with *Torpedo* D*72*G relative to those of the wild-type enzymes, in reasonable agreement with the 35-fold increase reported in mouse D74N (*14*).

Phosphorylation of Recombinant Human D74G by EMPC and DEPQ in the Presence and Absence of Peripheral Site Ligands. EMPC and DEPQ are fluorogenic OPs that release fluorescent leaving groups when they phosphorylate the AChE acylation site (Scheme 1). As observed previously with wild-type human AChEs (*9*), most of the fluorescence increase on reaction of these OPs with the human D74G mutant occurred with a single rapid exponential time course (data not shown). The dependence of the rate constants on the OP concentrations was analyzed with eq 8. The D74G mutation had little effect on the reaction of EMPC, a neutral OP. The first-order rate constant k_{OP} decreased about 2-fold, and the equilibrium dissociation constant K_{OP} decreased about 4-fold relative to that of wild-type AChE (Table 2). A similar decrease in k_{OP} was observed for DEPQ, a cationic OP, but K_{OP} increased by about an order of magnitude. These changes are consistent with those reported in second-order phosphorylation rate constants (k_{OP}/K_{OP}) for other neutral and cationic OPs with mouse wild-type and D74N AChEs (*16*). These reports showed that k_{OP}/K_{OP} for cationic OPs decreased 35−145-fold in the mutant relative to that of wild-type AChE, in contrast to a 1.4−2.6-fold increase for neutral OPs, and the authors concluded that D74 was responsible for the enhanced reactivity of cationic OPs relative to their uncharged counterparts.

In the presence of peripheral site ligands, interpretation of k_{OP} and K_{OP} in terms of the intrinsic rate constants in Scheme 1 involved extrapolation to a saturating concentration of the ligand (*9*). Since the extrapolation required a known K_I for the ligand, we determined K_I values of 29.5 ± 0.4 μM for propidium and 8.2 ± 0.6 nM for fasciculin 2 with human D74G AChE. These values are about 30- and 300-fold higher, respectively, than the corresponding K_I determinations with wild-type human AChE (*7*, *11*). These increases are somewhat larger than the respective 4- and 30-fold increases in K_I relative to that of the wild type previously reported for propidium and fasciculin 2, with mouse D74N AChE (*14*, *31*). The relatively low affinities of propidium and fasciculin 2 with human D74G AChE made it difficult to extrapolate their precise effects on OP phosphorylation, particularly with DEPQ. Propidium showed no inhibition of the EMPC reaction with this mutant, and both k_{OP} and K_{OP} increased when propidium was introduced (Table 2). The absence of propidium inhibition of EMPC phosphorylation also was seen with wild-type AChE (Table 2) and was noted previously to be consistent with our steric blockade model (*9*). Since this model predicts that a small peripheral site ligand like propidium will have relatively little effect on a substrate like an OP that equilibrates with the acylation site before acylation occurs, the increases in k_{OP} and K_{OP} might appear to require an additional conformational effect induced by bound propidium on the OP reactivity at the acylation site (*32*). However, these increases may arise simply from the fact that steric overlap would occur if both propidium and EMPC or DEPQ were placed in their normal binding sites in the binary AChE complexes (*9*). Molecular movement of the substrate to reduce this overlap can explain the increase in K_{OP} for both EMPC and DEPQ when propidium is bound with either wild-type or D74G AChE (Table 2), and this movement could induce strain in the bond to the OP leaving group to account for the increase in k_{OP} for EMPC (Table 2; *9*). Alternatively, this increase in k_{OP} may result from nonproductive binding of EMPC to the free enzyme, for example, with its leaving group directed inward rather than out of the active site gorge. If bound propidium interfered with EMPC binding in a nonproductive binding

configuration and thereby increased the percentage of EMPC bound in a productive mode, an increase in a (along with a corresponding increase in K_{OP}) would be expected, as seen in Table 2 for the propidium−EMPC ternary complexes. In any event, it is clear that there are mechanisms which could account for this increase in k_{OP} without invoking a propidium-induced conformational change in the acylation site.

In contrast to propidium, fasciculin 2 binding to the peripheral site dramatically decreased the phosphorylation rate constants for EMPC and DEPQ with wild-type AChE by 3−5 orders of magnitude (*9*; Table 2). We interpreted this qualitative difference from propidium to indicate that fasciculin induces a conformational change or a conformational restraint in the acylation site that reduces a (*9*). The D74G mutation appears to have an effect on the ability of fasciculin to induce this conformational change with EMPC. The value of a increased from 0.002 in the wild-type enzyme to 0.24 in D74G AChE (Table 2). Fasciculin 2 clearly inhibited the reaction of DEPQ with D74G AChE, but the maximal inhibition could not be determined. Estimates of k_{OP}/K_{OP} decreased nearly linearly with the fasciculin 2 concentration up to 10 μM, the highest concentration tested (Table 2). Because of the relatively low affinity of fasciculin 2 for the D74G enzyme, the residual free AChE dominated the reaction with DEPQ and prevented extrapolation to the very low rate constants for the reaction of DEPQ with the fasciculin 2 complex.

DISCUSSION

To understand the role of an active site residue in the AChE catalytic pathway, it is useful to determine the contribution of the residue to the affinity of substrates for the peripheral site. While this contribution can be assessed by measurements of K_S from substrate competition with fasciculin as depicted in Figure 1B, such measurements require great precision as well as a high affinity of fasciculin for the peripheral site. To develop an alternative procedure for measuring K_S in AChE mutants as well as in *Drosophila* AChE and BChE with low fasciculin affinities, we examined whether K_S can be measured directly from substrate inhibition curves as shown in Figure 1A. We show in Table 1 that K_S values can be obtained from substrate inhibition curves that agree with those from fasciculin competition if three conditions are met: (1) k_{cat} is determined independently from active site titrations; (2) K_{app} and $[E]_{tot}$ are estimated from an initial fit of the substrate inhibition curve to the Haldane equation (eq 1); and (3) simplifying assumptions are applied to Scheme 3 to decrease the independent rate constants to a number that can be fitted uniquely by a computer-assisted simultaneous equation solver. We impose the simplifying assumptions that several rate constants are unaffected by bound ligands (e.g., $a = b = 1$), are related by previous measurements in the literature (e.g., $k_2 = k_3$), or can be combined into terms (e.g., B and R/R_S) for which K_S is relatively insensitive. As future studies fit multiple v versus [S] data sets with, for example, varying concentrations of specific inhibitors, the number of independent rate constants that can be fitted uniquely should increase and eliminate uncertainties arising from the simplifying assumptions.

As a negatively charged residue in the AChE active site, D*72* in principle could affect catalytic activity in several ways. First, it could contribute to a general electrostatic effect that attracts cationic substrates and inhibitors. A high net negative charge near the active site was initially demonstrated by the effects of ionic strength on k_{cat}/K_{app} for cationic substrates and on the association rate constant k_I for cationic inhibitors (*33*). Molecular modeling calculations (*34*, *35*) from the three-dimensional structure supported this notion by suggesting that the AChE catalytic subunit has a dipole moment aligned with the active site gorge that accelerates association rates for cationic ligands. The magnitude of the acceleration can be estimated as the ratio of k_I extrapolated to zero ionic strength to k_I at high ionic strength. For example, this ratio was about 7.5 for the cationic trifluoromethyl ketone TMTFA and mouse AChE (*31*). It remained about 7.1 following mutation of D74 to N, even though this mutation decreased k_I for TMTFA more than 20-fold relative to that of wild-type AChE (*31*). From this comparison, we conclude that D*72* contributes very little to a general electrostatic effect on cationic ligands. This conclusion is consistent with other observations which show that negatively charged residues at or near the peripheral site contribute only modestly to the electrostatic field at the active site (*31*, *36*).

A second way in which D*72* could affect catalytic activity was recently proposed from molecular modeling studies of AChE (*37*). In these Brownian dynamics simulations, the mutation D74N had little effect on the frequency of cation entry into the peripheral site but significantly decreased the likelihood that a cation in the peripheral site would move to the acylation site. The simulations predicted a 30-fold reduction of k_I for TMTFA in the D74N mutant relative to that of the wild-type enzyme, in excellent agreement with the observed 25-fold reduction. These authors proposed that D*72* may act as an electrostatic anchor that traps cationic ligands entering the active site gorge (*37*). A similar proposal based on modeling calculations also has been offered (*38*). Our data provide strong experimental support for this hypothesis by showing that D*72* is directly involved in a transient binding of acetylthiocholine at the peripheral site. It is likely that as a consequence of this binding k_{-S} falls below k_1 in Scheme 3, ensuring that most substrate molecules that encounter the peripheral site proceed on to hydrolysis. Estimates of K_S, the equilibrium dissociation constant for this binding, can be obtained directly from the partially competitive effect of acetylthiocholine on fasciculin binding, and they can also be obtained indirectly by the application of Scheme 3 to the substrate inhibition curve for acetylthiocholine (Figure 1). Both methods agreed that K_S increased from about 1−2 mM in wild-type human AChE to about 30 mM in the D74G mutant.

The hypothesis that D*72* traps entering cationic ligands revives the classic notion of an anionic site in the AChE catalytic pathway (*10*) and suggests that D*72* functions as such a site. While K_S is the most direct measure of cationic substrate affinity for this anionic site, analysis according to Scheme 3 indicates that two parameters determined from eq 1, K_{app} and K_{SS}, are closely related to K_S. As noted above, mutation of D*72* to G decreased k_{cat}/K_{app} by increasing the effective K_{app} without appreciable effect on k_{cat}. Mutation of D*72* to G also increased the K_{SS} for acetylthiocholine and made substrate inhibition less evident. K_{SS} increased in the mutant because the level of substrate binding that gave rise to steric blockade was decreased. Therefore, according to

Scheme 3, mutations such as that in D*72*G that result in an increase in the K_S for substrate binding in the peripheral site (without an effect on k_{cat}) should give rise to parallel increases in K_{app} and K_{SS}. Furthermore, this loss in affinity should also be reflected in increases in K_I for cationic inhibitors specific to either the peripheral site or the acylation site, as shown by consideration of Scheme 4.

Scheme 4

$$E + I \underset{k_{-I1}}{\overset{k_{I1}}{\rightleftharpoons}} EI_P \underset{k_{-I2}}{\overset{k_{I2}}{\rightleftharpoons}} EI$$

In Scheme 4, an inhibitor first binds to the peripheral site with an equilibrium dissociation constant K_{I1}. Its partitioning between the peripheral site and the acylation site is then given by the equilibrium constant K_{I2} ($=k_{-I2}/k_{I2}$). The experimental $K_I = K_{I1}K_{I2}/(1 + K_{I2})$, and the inhibitor will be specific for the peripheral site if $K_{I2} \gg 1$ ($K_I = K_{I1}$) or for the acylation site if $K_{I2} \ll 1$ ($K_I = K_{I1}K_{I2}$). In either case, K_I is proportional to K_{I1}, and a mutation like that in D*72*G which we propose to increase only K_{I1} will increase the experimental K_I. Scheme 4 is consistent with experimental results. Mutations of D74 to G or N in human or mouse AChE consistently reduced the affinity of both monoquaternary ligands specific to the acylation site (edrophonium) and of cationic ligands specific to the peripheral site (propidium) by factors of about 5 (*14*, *31*, *39*). Bisquaternary ligands that bind simultaneously to both the peripheral and acylation sites are particularly sensitive to these D*72* mutations and showed reductions in affinity of more than 2 orders of magnitude. K_{OP} for OPs is essentially an equilibrium constant equivalent to a K_I, and Table 2 shows that K_{OP} for cationic DEPQ increased about 12-fold for human D74G relative to that for wild-type AChE. Similar decreases in the affinity of cationic ligands for the active site of BChE were observed when D70 was mutated to G (*17*). The affinity of monoquaternary cations decreased about 10-fold relative to that of the wild-type BChE, and that of bisquaternary cations decreased about 100-fold in the D70G mutant relative to that of the wild-type BChE. To account for these data, Masson et al. (*17*) proposed a mechanism in which a cationic ligand first binds to D70 before proceeding to a second site at the base of the active site gorge. Although no data were presented to demonstrate ligand binding near D70, this proposal is very similar to that inferred here for the role of D*72* in AChE.

A third possible way that D*72* could affect catalytic activity is by mediating a conformational change to the acylation site when a ligand binds to the peripheral site. Such a conformational change has been proposed previously to account for inhibition of substrate hydrolysis by bound peripheral site ligands (*17*, *40*), but in our view, solid evidence supporting this proposal has been obtained for only one peripheral site ligand, fasciculin (*9*). The binding of fasciculin drastically decreased organophosphorylation rate constants for both the neutral EMPC and the cationic DEPQ by factors of nearly 10^3-10^5 (Table 2). Since OPs essentially equilibrate prior to phosphorylation of S*200* in the acylation site (*9*), this inhibition cannot result from steric blockade. We previously rationalized this unique effect of fasciculin (*9*) by referring to crystal structure analyses of fasciculin−AChE complexes (*12*, *13*). These analyses show that fasciculin 2 interacts not only with W*279* and other residues in the peripheral site but also with residues on the outer surface of the C*67*−C*94* ω-loop within 4 Å of W*84* in the acylation site, well beyond the region of the peripheral site occupied by propidium (*7*, *15*). These more extensive surface interactions provide a structural basis for an inhibitory conformational effect on the acylation site when fasciculin but not propidium is bound to the peripheral site. Data in Table 2 indicate that some of this inhibitory conformational effect is mediated by D*72*. In particular, the first-order phosphorylation rate constant in the *E*OPXI$_P$ ternary complex with fasciculin relative to the corresponding rate constant in *E*OPX alone is given by the constant *a* in Scheme 1, and the low value of *a* for the wild-type enzyme (0.002) is a direct indication of the inhibitory conformational effect of fasciculin. Since *a* for EMPC increased about 100-fold to 0.24 in the human D74G mutant relative to that in wild-type AChE, almost all of the inhibitory effect of fasciculin on first-order phosphorylation by EMPC was lost in the mutant. Therefore, even though D*72* does not make direct contact with fasciculin 2 according to the crystal structures, it may be important in maintaining an interaction between fasciculin and the ω-loop that is necessary to transmit the inhibitory conformational effect. Evidence supporting a role for D*72* in this interaction was provided by the 300-fold decrease in fasciculin 2 affinity in the human D74G mutant relative to that in the wild-type enzyme.

ACKNOWLEDGMENT

We are grateful to Drs. Suzanne Bon and Jean Massoulié (CNRS URA 1857, Paris, France) for the construction and expression of the *Torpedo* AChEs. We thank Dr. Pascale Marchot (CNRS Unite Propre de Recherche 9039, Marseille, France) for a sample of highly purified fasciculin 3 (*23*).

REFERENCES

1. Rosenberry, T. L. (1979) *Biophys. J. 26*, 263−290.
2. Rosenberry, T. L. (1975) Acetylcholinesterase. In *Advances in Enzymology* (Meister, A., Ed.) Vol. 43, pp 103−218, John Wiley & Sons, New York.
3. Taylor, P., and Lappi, S. (1975) *Biochemistry 14*, 1989−1997.
4. Sussman, J. L., Harel, M., Frolow, F., Oefner, C., Goldman, A., Toker, L., and Silman, I. (1991) *Science 253*, 872−879.
5. Velan, B., Barak, D., Ariel, N., Leitner, M., Bino, T., Ordentlich, A., and Shafferman, A. (1996) *FEBS Lett. 395*, 22−28.
6. Ollis, D. L., Cheah, E., Cygler, M., Dijkstra, B., Frolow, F., Franken, S. M., Harel, M., Remington, S. J., Silman, I., Schrag, J., Sussman, J. L., Verschueren, K. H. G., and Goldman, A. (1992) *Protein Eng. 5*, 197−211.
7. Szegletes, T., Mallender, W. D., and Rosenberry, T. L. (1998) *Biochemistry 37*, 4206−4216.
8. Szegletes, T., Mallender, W. D., Thomas, P. J., and Rosenberry, T. L. (1999) *Biochemistry 38*, 122−133.
9. Mallender, W. D., Szegletes, T., and Rosenberry, T. L. (1999) *J. Biol. Chem. 274*, 8491−8499.
10. Nachmansohn, D., and Wilson, I. B. (1951) *Adv. Enzymol. 12*, 259−339.
11. Eastman, J., Wilson, E. J., Cervenansky, C., and Rosenberry, T. L. (1995) *J. Biol. Chem. 270*, 19694−19701.
12. Harel, M., Kleywegt, G. J., Ravelli, R. B. G., Silman, I., and Sussman, J. L. (1995) *Structure 3*, 1355−1366.
13. Bourne, Y., Taylor, P., and Marchot, P. (1995) *Cell 83*, 503−512.
14. Radic, Z., Pickering, N. A., Vellom, D. C., Camp, S., and Taylor, P. (1993) *Biochemistry 32*, 12074−12084.

15. Barak, D., Kronman, C., Ordentlich, A., Ariel, N., Bromberg, A., Marcus, D., Lazar, A., Velan, B., and Shafferman, A. (1994) *J. Biol. Chem. 269*, 6296−6305.
16. Hosea, N. A., Radic, Z., Tsigelny, I., Berman, H. A., Quinn, D. M., and Taylor, P. (1996) *Biochemistry 35*, 10995−11004.
17. Masson, P., Legrand, P., Bartels, C. F., Froment, M.-T., Schopfer, L. M., and Lockridge, O. (1997) *Biochemistry 36*, 2266−2277.
18. Kalow, W. (1962) *Pharmacogenetics: heredity and the response to drugs*, pp 69−136, W. B. Saunders Co., Philadelphia.
19. Lockridge, O. (1990) *Pharmacol. Ther. 47*, 35−60.
20. Rosenberry, T. L., and Scoggin, D. M. (1984) *J. Biol. Chem. 259*, 5643−5652.
21. Duval, N., Bon, S., Silman, I., Sussman, J., and Massoulié, J. (1992) *FEBS Lett. 309*, 421−423.
22. Harel, M., Sussman, J. L., Krejci, E., Bon, S., Chanal, P., Massoulié, J., and Silman, I. (1992) *Proc. Natl. Acad. Sci. U.S.A. 89*, 10827−10831.
23. Marchot, P., Khelif, A., Ji, Y.-H., Masnuelle, P., and Bourgis, P. E. (1993) *J. Biol. Chem. 268*, 12458−12467.
24. Karlsson, E., Mbugua, P. M., and Rodriguez-Ithurralde, D. (1984) *J. Physiol. (Paris) 79*, 232−240.
25. Laemmli, U. K. (1970) *Nature 227*, 680−685.
26. Ellman, G. L., Courtney, K. D., Andres, J. V., and Featherstone, R. M. (1961) *Biochem. Pharmacol. 7*, 88−95.
27. Riddles, P. W., Blakeley, R. L., and Zerner, B. (1979) *Anal. Biochem. 94*, 75−81.
28. Haldane, J. B. S. (1930) *Enzymes*, p 84, Longman, New York.
29. Froede, H. C., and Wilson, I. B. (1984) *J. Biol. Chem. 259*, 11010−11013.
30. Bazelyansky, M., Robey, E., and Kirsch, J. F. (1986) *Biochemistry 25*, 125−130.
31. Radic, Z., Kirchhoff, P. D., Quinn, D. M., McCammon, J. A., and Taylor, P. (1997) *J. Biol. Chem. 272*, 23265−23277.
32. Radic, Z., and Taylor, P. (1999) *Chem.-Biol. Interact. 119−120*, 111−117.
33. Nolte, H. J., Rosenberry, T. L., and Neumann, E. (1980) *Biochemistry 19*, 3705−3711.
34. Ripoll, D. R., Faerman, C. H., Axelsen, P. H., Silman, I., and Sussman, J. L. (1993) *Proc. Natl. Acad. Sci. U.S.A. 90*, 5128−5132.
35. Antosiewicz, J., McCammon, J. A., Wlodek, S. T., and Gilson, M. K. (1995) *Biochemistry 34*, 4211−4219.
36. Shafferman, A., Ordentlich, A., Barak, D., Kronman, C., Ber, R., Bino, T., Ariel, N., Osman, R., and Velan, B. (1994) *EMBO J. 13*, 3448−3455.
37. Tara, S., Elcock, A. H., Kirchhoff, P. D., Briggs, J. M., Radic, Z., Taylor, P., and McCammon, J. A. (1998) *Biopolymers 46*, 465−474.
38. Botti, S. A., Felder, C. E., Lifson, S., Sussman, J. L., and Silman, I. (1999) *Biophys. J. 77*, 2430−2450.
39. Shafferman, A., Velan, B., Ordentlich, A., Kronman, C., Grosfeld, H., Leitner, M., Flashner, Y., Cohen, S., Barak, D., and Ariel, N. (1992) *EMBO J. 11*, 3561−3568.
40. Barak, D., Ordentlich, A., Bromberg, A., Kronman, C., Marcus, D., Lazar, A., Ariel, N., Velan, B., and Shafferman, A. (1995) *Biochemistry 34*, 15444−15452.

BI000210O